

# Heat Pipe and Surface Mass Transfer Cooling of Hypersonic Vehicle Structures

Gene T. Colwell\*

Georgia Institute of Technology, Atlanta, Georgia 30332  
and

James M. Modlin†

U.S. Army Strategic Defense Command, Huntsville, Alabama 35807

This paper describes the results of an investigation conducted to study the feasibility of cooling hypersonic vehicle leading-edge structures exposed to severe aerodynamic surface heat fluxes using a combination of liquid metal heat pipe and surface mass transfer cooling techniques. A generalized, transient, finite difference-based hypersonic leading-edge cooling model was developed that incorporated these effects and was demonstrated on an assumed aerospace plane-type wing leading-edge section. An existing experimentally verified heat pipe model was modified by adding both transpiration and film cooling options as new surface boundary conditions. The models used to predict the leading-edge surface heat transfer reduction effects of transpiration and film cooling were modifications of more generalized, empirical-based models obtained from the literature. The leading-edge cooling model was demonstrated on an assumed aerospace plane-type wing leading-edge section exposed to a severe laminar, hypersonic aerodynamic surface heat flux. A 1-in.-nose diameter leading-edge structure was cooled using a lithium-filled heat pipe supplemented by either surface transpiration, surface film, or internal active heat exchanger cooling while executing a 2000 psf constant dynamic pressure hypersonic ascent flight trajectory. Results included transient structural temperature distributions, transient aerodynamic heat inputs, and transient surface coolant distributions. The study indicated that these cooling techniques limited the maximum leading-edge surface temperatures, moderated the structural temperature gradients, and led to the conclusion that cooling leading-edge structures exposed to severe hypersonic flight environments using a combination of liquid metal heat pipe, surface transpiration, and film cooling methods appeared feasible.

## Nomenclature

$C$	= specific heat
$C_p$	= constant pressure specific heat, kJ/kg·K
$c_f$	= coefficient of friction
$k$	= thermal conductivity, W/m·K
$L$	= length in chord direction, m
$M$	= molecular weight, kg/k mole
$\dot{m}$	= mass flow rate, kg/s
$Pr$	= Prandtl number
$Q$	= thermal transport, W
$q$	= heat flux, W/m <sup>2</sup>
$Re$	= Reynolds number
$St$	= Stanton number
$T$	= temperature, K
$t$	= time, s
$u$	= chord direction velocity
$v$	= surface normal direction velocity
$X$	= chord direction, m
$Y$	= normal direction, m
$Z, z$	= span direction, unit span length, m
$\epsilon$	= emissivity
$\theta$	= wedge angle
$\mu$	= dynamic viscosity, N·s/m <sup>2</sup>
$\rho$	= density, kg/m <sup>3</sup>
$\sigma$	= Stefan Boltzmann constant, W/m <sup>2</sup> ·K <sup>4</sup>

## Subscripts

1	= skin
---	--------

2	= capillary structure
AERO	= aerodynamic
air	= air property
cool	= coolant property
$e$	= boundary-layer edge condition
HX	= heat exchanger
0	= no surface cooling
os	= outer surface
RAD	= radiant
$r$	= recovery condition
STAG	= stagnation condition
scs	= skin/capillary structure interface
$V$	= vapor
$V_{IN}$	= into vapor
$V_{OUT}$	= from vapor
$w$	= wall/surface condition
$\infty$	= surroundings

## Introduction

AS hypersonic aircraft travel through the Earth's atmosphere during ascent, reentry, or cruise portions of a flight, aerodynamic heating may become so intense near leading edges of wings, fuselages, and engine inlets that skin materials must be protected or cooled. Several methods of cooling and protection are possible for various surface geometries. Thermal barrier coatings, such as ceramic materials, can be attached to outer skins.<sup>1</sup> Internal convective cooling can be used where a fluid is circulated through tubes or channels within the structure.<sup>2</sup> Fluids can be used for surface transpiration cooling, and ablative materials can be attached to the surface for cooling.<sup>3,4</sup> Another suggested concept is to place a heat pipe inside the hot structure where heating is most intense.<sup>5</sup> The effect of the heat pipe is to transfer heat internally from the area of intense heating to regions of lower heating, thereby reducing maximum skin temperatures and thermal gradients. It appears, however, that combinations of

Received Dec. 20, 1990; revision received June 20, 1991; accepted for publication July 14, 1991. Copyright © 1991 by the American Institute of Aeronautics and Astronautics, Inc. All rights reserved.

\*Professor.

†Major, P.O. Box 1500.

these cooling and protection schemes will be required for some of the future air-breathing, low-drag configuration hypersonic aircraft missions now being considered.<sup>6</sup> As an example, for the "National Aerospace Plane" (NASP) the maximum aerodynamic heating near the wing stagnation point occurs during ascent and is on the order of  $10^4$  kW/m<sup>2</sup>, almost two orders of magnitude greater than the maximum stagnation heat flux experienced by the Space Shuttle wing.<sup>7</sup> To date, there appears to be no singular cooling method capable of protecting leading-edge structures from aerodynamic heat fluxes of this magnitude. Thus, there exists a need to investigate the feasibility of incorporating combinations of surface cooling techniques for a NASP-type hypersonic vehicle leading-edge structure.

The objective of this article is to present the results of a numerical study of the transient thermal behavior of hypersonic aircraft leading-edge structures which are cooled using a combination of liquid metal heat pipes, internal active heat exchangers through which a coolant liquid or vapor is circulated, and surface mass transfer cooling.

### Leading-Edge Cooling Model

Figure 1 shows a schematic of a heat pipe-cooled leading edge with an internal active heat exchanger. Aerodynamic heating occurs on the outer skin. Some of this energy is conducted through the skin into the vapor interior of the heat pipe, and some is directly radiated away. Some of the heat conducted into the heat pipe evaporator section may be taken away by the active heat exchanger. The remainder is transferred through the heat pipe vapor interior to the condensing region, conducted to the outer skin surface, then radiated away. The portion of the heat pipe which acts as the evaporator section changes as the aerodynamic heating and active coolant flow are changed. For situations where heating is very large, such as during the peak heating portion of a typical NASP ascent flight, a significant active coolant flow is required to keep skin temperatures below a maximum acceptable level. The entire capillary structure on the inside of the skin may operate in an evaporative mode with condensation occurring on the active heat exchanger surface. The heat pipe working fluid must then be returned to the evaporator surface by additional capillary action or other means. When the cooled leading-edge region is operated in this manner, a small portion of the aerodynamic heating is directly radiated away and the remaining larger portion is transferred through the skin into the interior where it is taken away by the active coolant. It should be noted that for all situations heat fluxes and temperatures are changing with time, and, thus, some thermal energy will be absorbed or supplied by the various masses in the structure due to their heat storage capacities.

Figure 2 shows how aerodynamic heating varies with chordwise distance from the leading edge. The shape of this curve changes significantly as the shape of the structure's leading-edge changes.<sup>8</sup> Figure 3 shows how the stagnation point heat flux changes with time during an ascent mission.<sup>9</sup> Mathematical models have been developed which predict detailed transient temperature distributions throughout aircraft structures as well as heat fluxes and heat pipe fluid properties.<sup>10-14</sup>

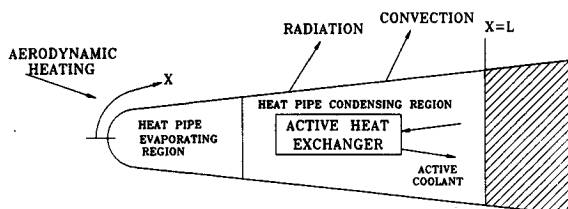


Fig. 1 Schematic of a heat pipe-cooled hypersonic aircraft leading edge.

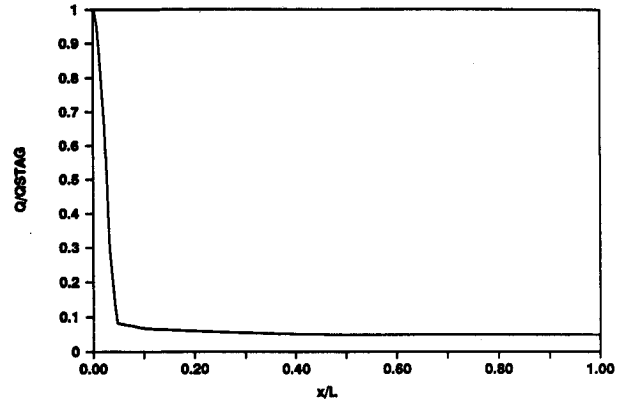


Fig. 2 Aerodynamic heat flux surface distribution.

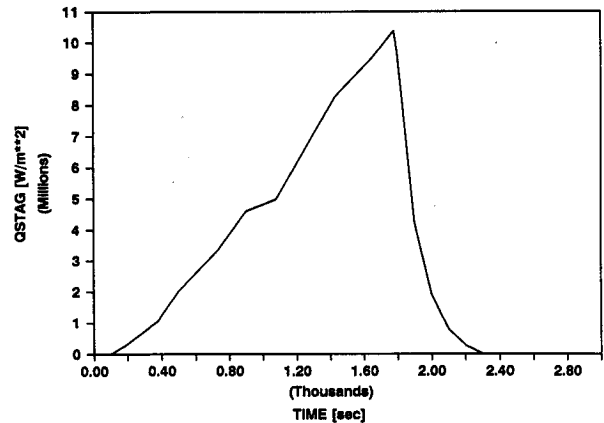


Fig. 3 Transient stagnation aerodynamic heat flux.

### Heat Pipe Model

A finite difference model was used in this study which incorporated aerodynamic heating that varied with time and chordwise position, radiation, or convection interchange with the surroundings, time-varying active heat exchanger cooling, and temperature-varying thermal properties. It was based upon the following assumptions<sup>12</sup>:

- 1) Heat transfer through the heat pipe wall and capillary structure was by conduction only.
- 2) There were negligible thermal resistances at the liquid/vapor interfaces in the evaporator and condenser sections.
- 3) There were negligible thermal resistances in the vapor space, thus the vapor temperature was spatially uniform and varied only with time.
- 4) Spanwise temperature gradients along the leading edge were neglected.
- 5) The temperature distribution of the leading edge was symmetric about the stagnation point.
- 6) Surface curvature was neglected.
- 7) The working fluid was operating in continuum flow regime, thus no startup effects were considered.

Referring to Fig. 4, the various regions were mathematically described as:

- 1) Skin Conduction

$$\frac{\partial(\rho_1 C_1 T_1)}{\partial t} = \nabla \cdot [k_1 \nabla T_1] \quad (1)$$

where  $T_1 = T_1(t, X, Y)$ .

- 2) Capillary Structure

$$\frac{\partial(\rho_2 C_2 T_2)}{\partial t} = \nabla \cdot [k_2 \nabla T_2] \quad (2)$$

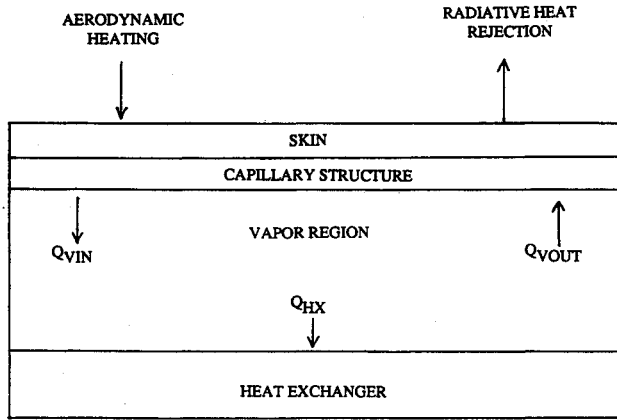


Fig. 4 Heat pipe cooling model energy balance.

where  $T_2 = T_2(t, X, Y)$  and properties were effective properties that accounted for working fluid properties, capillary structure properties, porosity, and temperature.

### 3) Vapor Region

$$-L \int_0^1 k_2 \frac{\partial T_2}{\partial Y} \bigg|_v d\left(\frac{x}{L}\right) = Q_{HX} + \frac{1}{L} \frac{\partial(m_{HX} C_{HX} T_V)}{\partial t} \quad (3)$$

where  $T_V = T_V(t)$

### 4) Outer Surface

$$Q_{AERO} - Q_{RAD} + L \int_0^1 k_1 \frac{\partial T_1}{\partial Y} \bigg|_{os} d\left(\frac{x}{L}\right) = 0 \quad (4)$$

where

$$Q_{AERO} = L q_{STAG} \int_0^1 \frac{q}{q_{STAG}} d\left(\frac{x}{L}\right) \quad (5)$$

$$Q_{RAD} = L \int_0^1 \epsilon \sigma (T_{1,os}^4 - T_\infty^4) d\left(\frac{x}{L}\right) \quad (6)$$

and emissivity and absorptivity of the wing outer surface were assumed to be equal.

### 5) Skin/Capillary Structure Interface

$$-k_1 \frac{\partial T_1}{\partial Y} \bigg|_{scs,x} = -k_2 \frac{\partial T_2}{\partial Y} \bigg|_{scs,x} \quad (7)$$

Finite difference equations, logic schemes and computer programs have been developed, based upon these governing equations and assumptions, which predict transient thermal behavior of the structures under consideration.<sup>12</sup>

Camarda and Masek<sup>15</sup> built and tested a model of a Space Shuttle-type wing with internal sodium heat pipes. They measured transient thermal performance under a variety of heating conditions. Their experimental results compare well to predicted surface temperatures computed using both a finite element model described by Colwell, et al.,<sup>11</sup> and the finite difference model described above. The computed maximum temperatures, however, were somewhat above the measured values of Camarda and Masek,<sup>15</sup> largely because convective cooling, which existed in their experiments, was not accounted for in the computations and because the emissivity of the test surface was not reported. Assumed emissivity values of 0.8 and 0.85 were used in the computations.

The finite element and finite difference computations also compared well with each other as temperatures reached a maximum at the stagnation point but, as expected, differed greatly at intermediate times, from 0–800 s for the conditions shown on Fig. 3, during heat pipe startup.<sup>14</sup> These differences occurred due to working fluid melting, transition from free

molecular to continuum flow, and choking conditions which are included in the finite element model but are not included in the finite difference model. A rather minor amount of the difference can be attributed to curvature effects which are only considered in the finite element model.

## Surface Mass-Transfer Model

As a proven technology for cooling missiles and re-entry vehicles, mass-transfer cooling techniques, transpiration, and film and ablation cooling are well documented in the literature.<sup>16–20</sup> However, there is no published account of investigating the effect of these surface cooling techniques in conjunction with heat pipe hypersonic surface leading-edge cooling techniques. Consequently, the finite difference heat pipe model described above was modified to account for surface transpiration and film-cooling effects. Ablative cooling was not considered in this application due to its characteristic problems of the surface refurbishment/replacement of the ablative material after a mission and the potential in flight vehicle stability/control concerns due to changing leading-edge geometry and surface roughness resulting from the ablative process. However, an interesting solution to the changing leading-edge geometry problem has been presented by Camberos and Roberts.<sup>4</sup>

Transpiration cooling refers to the continuous injection of a coolant fluid through a porous surface. Film cooling refers to the continuous injection of a coolant fluid through discrete slots or holes in the surface (see Fig. 5). The surface protection effect of these methods is a combination of heat absorption by the coolant fluid and a heat transfer blocking action by the coolant as it sweeps over the surface. The presence of the coolant in the boundary layer and near the surface serves to reduce the temperature and velocity gradients at the surface, thus reducing the heat transfer rate to the surface.

Several researchers have investigated the complicated and detailed flow phenomena associated with mass-addition into hypersonic laminar and turbulent boundary layers analytically, numerically, and experimentally.<sup>21–26</sup> Reported results have generally been based on known isothermal or adiabatic surface conditions, or on computationally intensive numerical solutions of the boundary-layer equations modified to account for surface mass-addition effects. The hypersonic aircraft leading edge surface studied in this investigation, on the other hand, had a transient, unknown surface temperature distribution and was not adiabatic (see Figs. 1–3). Furthermore, the interest of this study was on the heat pipe-cooled structural response to the aerodynamic heating/surface mass-transfer cooling effects, not on the detailed boundary-layer response to coolant mass injection. Thus, it was desired to model the surface mass-transfer cooling effects using simple expressions that approximated well the more exact predictions and experimental results. It was envisioned that such a cooling model

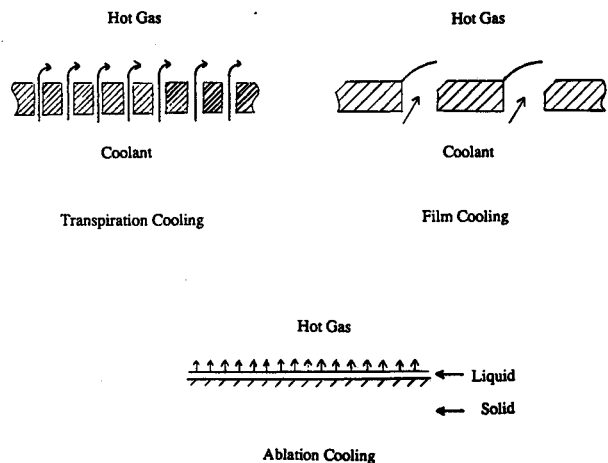


Fig. 5 Various mass-transfer surface cooling techniques.

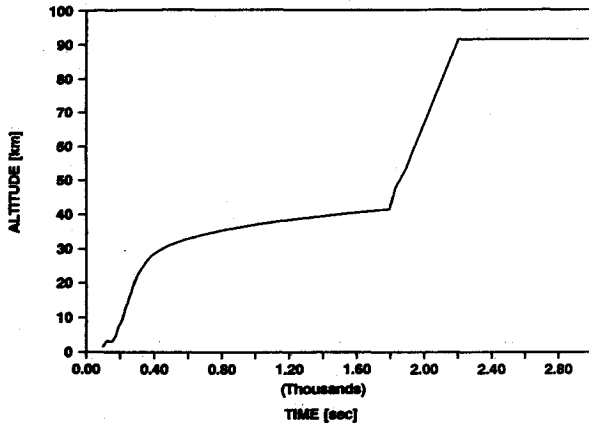


Fig. 6 Typical hypersonic aircraft flight trajectory.

would be of value for subsequent, more detailed engineering design calculations. The following additional model assumptions were made:

- 1) A detached shock was present upstream of the leading edge.
- 2) There was no shock/boundary-layer interaction and no shock/shock interference.
- 3) The flow field in the vicinity of the leading edge was represented as flow past a normal shock.
- 4) The air in this region was in local thermochemical equilibrium, and high-temperature gas effects were important.
- 5) Air properties at the surface boundary-layer edge were equal to those immediately after the shock.
- 6) Boundary-layer flow over the leading edge was laminar.

To examine the cooling model's application, a typical NASP-type hypersonic vehicle leading edge (see Figs. 1–3) was further defined by having the additional characteristics of a) a leading edge nose radius of 0.5 in.; b) a columbium alloy liquid metal heat pipe with length  $L$  of 16 in. and working fluid of lithium; c) a sweep angle of 70 deg and a wedge angle  $\theta$  of 7 deg; d) conducting a 2000-psf constant dynamic pressure ascent mission; e) executing the flight trajectory shown on Fig. 6; and f) all surface coolant fluids being gaseous.

### Transpiration Cooling

Gross et al.<sup>27</sup> developed a simple expression for predicting heat transfer reductions, in the presence of transpiration cooling, for laminar flow over a surface with zero pressure gradient. Their work was a result of an analysis that correlated the experimental results of earlier researchers by relating a normalized heat transfer reduction parameter  $q/q_0$  to a dimensionless mass transfer parameter  $J$

$$J = \left( \frac{\rho_w v_w}{\rho_e u_e} \right) \left( \frac{Re_x}{C^*} \right)^{1/2} \quad (8)$$

as

$$\frac{q}{q_0} = 1 - 1.82 \left( \frac{M_{air}}{M_{cool}} \right)^{1/3} \left( \frac{\rho_w v_w}{\rho_e u_e} \right) \left( \frac{Re_x}{C^*} \right)^{1/2} \quad (9)$$

where  $Re_x$  was based on boundary-layer edge conditions

$$C^* = \frac{\rho^* \mu^*}{\rho_e \mu_e} \quad (10)$$

and  $\rho^*$  and  $\mu^*$  were evaluated at the reference temperature  $T^*$  expressed as<sup>28</sup>

$$T^* = T_e + 0.72(T_r - T_e) \quad (11)$$

Gross et al.<sup>27</sup> also addressed the effect of pressure gradient on laminar mass-transfer cooling. The greatest reduction in

heat transfer occurs for the zero pressure gradient (flat plate condition), and the least reduction occurs for plane stagnation flow. However, for small values of the dimensionless mass transfer parameter  $J$  such as those used near the stagnation line of the present structure (see Table 1), the difference in heat transfer reduction between flat plate and plane stagnation flow is small. Therefore, based on this result, the structure's sharp nose radius/small wedge angle and the heat pipe-cooling model assumptions, the leading-edge surface in this study was modeled, for transpiration cooling, as a flat plate using Eq. (9) to predict the transpiration cooling effects.

Equation (9) can be expressed in terms of  $x/L$  as

$$\frac{q}{q_0} = 1 - 1.16 \left( \frac{M_{air}}{M_{cool}} \right)^{1/3} I \rho_e \left[ \frac{u_e}{(\rho \mu)^*} \right]^{1/2} \left( \frac{x}{L} \right)^{1/2} \quad (12)$$

where

$$I = \frac{\rho_w v_w}{\rho_e u_e} \quad (13)$$

Limitations of this model were twofold. First, Gross et al.<sup>27</sup> indicated that Eq. (9) is generally valid for the dimensionless mass-transfer parameter having an upper bound of 0.25 to 0.30 or

$$I \rho_e \left[ \frac{u_e}{(\rho \mu)^*} \right]^{1/2} x^{1/2} \leq 0.25 \quad (14)$$

$$I \leq \frac{0.25}{\rho_e} \left[ \frac{(\rho \mu)^*}{u_e} \right]^{1/2} x^{-1/2} \quad (15)$$

Thus, as seen in Eqs. (9) and (15), the dimensionless parameter  $I$  was a function of time and chordwise distance along the surface. In this study the distance dependency was selected to match the heat flux dependency (Fig. 2). The selected time dependency that satisfies Eq. (15) is shown in Fig. 7.

The second model limitation was a result of the velocity boundary-layer thickening due to mass addition. Excessive transpiration can lead to destabilization of the laminar bound-

Table 1 Cases considered

Time (s)	$x/L$	$I$	$Re_x^b$	$J$	$K$
900	0.0001*	0.01	10	0.031	0.031
	0.001	0.00995	98		0.100
	0.0025	0.00995	244		0.155
	0.0125	0.0087	1219		0.304
	0.0425	0.0014	4145		0.090
	1.0	0.005	$9.75 \times 10^4$		0.156
	1.0	0.001	6		0.156
1430	0.0001*	0.02	6	0.049	0.049
	0.001	0.0199	61		0.155
	0.0025	0.0199	152		0.246
	0.0125	0.0174	762		0.480
	0.0425	0.0028	2591		0.143
	1.0	0.001	$6.10 \times 10^4$		0.247
	1.0	0.001	5		0.247
1780	0.0001*	0.02	5	0.046	0.046
	0.001	0.0199	53		0.145
	0.0025	0.0199	132		0.229
	0.0125	0.174	660		0.447
	0.0425	0.0028	2245		0.133
	1.0	0.001	$5.28 \times 10^4$		0.230
	1.0	0.001	5		0.230
1900	0.0001*	0.02	0.5	0.014	0.014
	0.001	0.0199	5		0.044
	0.0025	0.0199	12		0.061
	0.0125	0.174	61		0.136
	0.425	0.0028	207		0.040
	1.0	0.001	4877		0.070
	1.0	0.001	4877		0.070

\*Represents approximate stagnation line condition.

<sup>b</sup>Based on boundary-layer edge conditions.

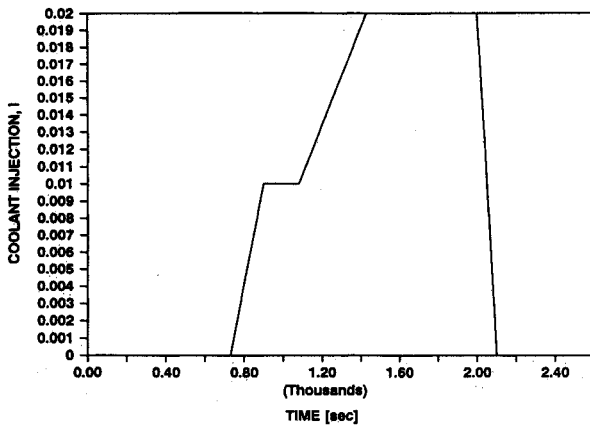


Fig. 7 Transpiration coolant injection profile.

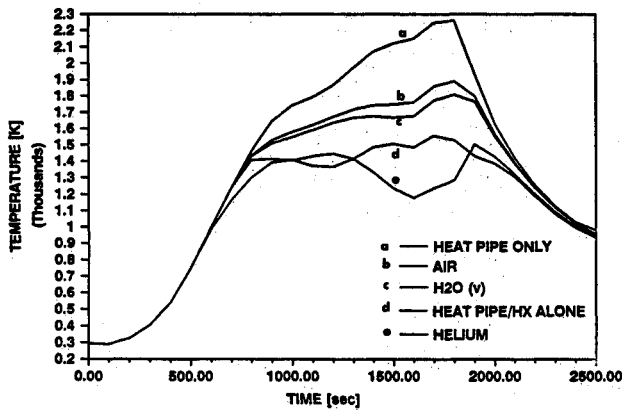


Fig. 8 Transient surface stagnation temperatures using transpiration cooling.

ary layer. For air injection it has been reported that this may occur when<sup>27</sup>:

$$K \equiv \left( \frac{\rho_w v_w}{\rho_e \mu_e} \right) Re_x^{1/2} = 0.619 \quad (16)$$

and lighter gases tend to be more destabilizing. As shown in Table 1, the values of  $K$  used in this study were well below 0.619.

The results of incorporating the transpiration cooling model with the existing heat pipe-cooled leading-edge finite difference model are shown in Fig. 8. In this figure the predicted transient surface stagnation temperatures for three gaseous coolants with no internal heat exchanger are given. For comparison, the stagnation temperature results for heat pipe cooling alone (no heat exchanger, no surface mass-transfer cooling) and for heat pipe with heat exchanger cooling (no mass-transfer cooling) are included. The heat exchanger heat load utilized is shown in Fig. 9.

It has been reported that the maximum allowable surface temperature of available aerostructural materials is approximately 1500–1800 K.<sup>1</sup> Given this criteria, it appears that under the conditions which yield the results of Fig. 8 heat pipe cooling alone is not sufficient from the ascent mission time of approximately 1000 to 2000 s. Heat pipe/heavy gas transpiration cooling are marginally sufficient during this time. Heat pipe cooling supplemented by an internal heat exchanger (defined by Fig. 9) or supplemented by a transpiring lightweight gas (helium in this study) appears to be fully adequate.

In order for the heavier transpiring gases (air and water vapor in this study) to be more effective, either an internal heat exchanger should be used in conjunction with the transpiration cooling or the amount of transpiration coolant injection should be increased. In the first option, the required

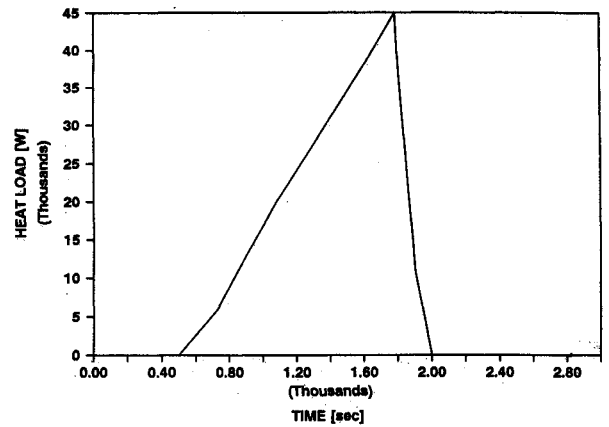


Fig. 9 Internal heat exchanger heat load.

internal heat exchanger heat load could be reduced from that shown in Fig. 9 and, subsequently, the heat exchanger coolant mass flowrate requirements. This would significantly lessen the heat exchanger design requirements. In the second option, the use of an internal heat exchanger is unnecessary. However, the amount of increase of transpiration coolant injection requires careful consideration. First, care must be taken to insure the laminar boundary layer is not destabilized due to the resultant increase of coolant mass into the boundary layer. If this destabilization occurs, the result would be a significant increase in heat transfer to the surface yielding higher surface temperatures than predicted. Second, the increase of coolant transpiration should not result in a condition which falls outside the limits of the Eq. (14).

### Film Cooling

Redeker and Miller<sup>29</sup> have shown good correlation between experimental and theoretical studies of laminar film cooling a 1-in. nose radius hemi-cylinder slab, approximating a full scale wing, in Mach 16 flow. Basing their analytical development on the discrete layer flow model of Papell and Hatch,<sup>30</sup> which they and others<sup>31</sup> have experimentally verified for laminar flow, Redeker and Miller developed the following relationship for the heat transfer reduction due to film cooling an isothermal, nonadiabatic surface

$$\frac{q_w}{q_0} = \frac{A}{1 + A} (1 - e^{-B}) \quad (17)$$

where

$$A = \left( \frac{M_{cool}}{M_{air}} \right)^{1/2} \frac{Cp_{cool}}{Cp_{air}} \quad (18)$$

and

$$B = \frac{2(1 + A)}{\left( \frac{\dot{m}}{z} Cp \right)_{cool}} \int_0^x h_a dx \quad (19)$$

The relationship between  $h_a$  (the heat transfer coefficient between the boundary-layer air and the coolant film being injected at the stagnation point) and surface distance  $x$  was determined experimentally by Redeker and Miller.<sup>29</sup> However, in the present study this functional relationship, the relationship between the boundary-layer-to-surface heat transfer coefficient and surface distance (the no injection case), was unknown, and the surface temperature distribution along the heat pipe-cooled leading edge was unknown, all due to a lack of available experimental data.

To overcome these shortcomings, the boundary-layer-to-coolant film heat transfer coefficient was first assumed to

Table 2 Predicted and measured heat transfer reductions

$x$	$\dot{w}_{cool}$	$= 0.26$	$\dot{w}_{cool}$	$= 0.66$	$\dot{w}_{cool}$	$= 0.018$	$\dot{w}_{cool}$	$= 0.028$
[m]	Ref. 29	Eq. (17)	Ref. 29	Eq. (17)	Ref. 29	Eq. (17)	Ref. 29	Eq. (17)
0.011	0.2	0.30	0.15	0.21	0.55	0.34	0.4	0.34
0.017	0.3	0.32	0.2	0.24	0.6	0.34	0.5	0.34
0.059	0.3	0.34	0.2	0.30	0.5	0.34	0.5	0.34
0.180	0.4	0.34	0.2	0.33	0.6	0.34	0.5	0.34

equal the boundary-layer-to surface heat transfer coefficient.<sup>32</sup> Second, it was assumed that the Reynolds analogy for laminar flow over a flat plate was valid for this situation:

$$StPr^{2/3} = (C_f/2) \quad (20)$$

Table 1 indicates, for the conditions of this study, that a laminar flow assumption in the vicinity of the leading edge of the structure depicted in Fig. 1 was reasonable. Additionally, it has been shown that the Reynolds analogy, developed from an incompressible flow analysis, gives reasonable approximations at hypersonic speeds and that these same physical trends hold for hypersonic boundary layers over general aerodynamic shapes.<sup>33</sup>

Thus, by employing these assumptions  $h_a$  in Eq. (19) may be written as

$$h_a = 0.332Re_x^{-1/2}Pr^{-2/3}\rho_e C_{pe}u_e \quad (21)$$

where all air properties were evaluated at the boundary layer edge condition. Further, to better approximate an actual compressible condition by the effective incompressible one, Eq. (21) can be modified as<sup>28</sup>

$$h_a^* = (\rho^*/\rho_e) \cdot h_a \quad (22)$$

$$h_a^* = 0.332Re_x^{*-1/2}Pr^{*-2/3}\rho^* C_{pe}u_e \quad (23)$$

where (\*) properties are determined from the reference temperature, Eq. (11), and the variation of  $Pr$  with  $Pr^*$  is considered small. Substituting Eq. (23) into Eq. (19) and simplifying yields

$$B = 1.68 \frac{(1 + A)}{\left(\frac{\dot{m}}{z}\right)_{cool}} \left(\frac{C_{p_{air}}}{C_{p_{cool}}}\right) [u_e(\rho\mu)^*]^{1/2} x^{1/2} \quad (24)$$

for  $Pr = 0.71$ .

Table 2 shows the results of comparing the predicted heat transfer reduction of Eq. (17), modified by Eq. (24) to the experimental results of Redeker and Miller<sup>29</sup> for various  $x$  locations along the surface and values of coolant mass flowrate per unit span length. As indicated in Fig. 2, the greatest amount of aerodynamic heating for the present structure occurs in the range of  $0 \leq x/L \leq 0.04$  which corresponds to  $0 \leq x \leq 0.016$  for  $L = 0.4064$  m (16 in.). Table 2 shows a good correlation between the Redeker and Miller<sup>29</sup> experimental data and the Eq. (17) predictions especially in the range of  $0 \leq x \leq 0.016$ .

Thus, Eqs. (17), (18), and (24) were used in the present study to model the heat transfer reduction due to laminar film cooling on the surface of the heat pipe-cooled leading edge of Fig. 1. Equation (24) was further modified to account for a  $x/L$  variation by

$$B = \frac{1.07}{\dot{w}_{cool}} (1 + A) \left(\frac{C_{p_{air}}}{C_{p_{cool}}}\right) [u_e(\rho\mu)^*]^{1/2} \left(\frac{x}{L}\right)^{1/2} \quad (25)$$

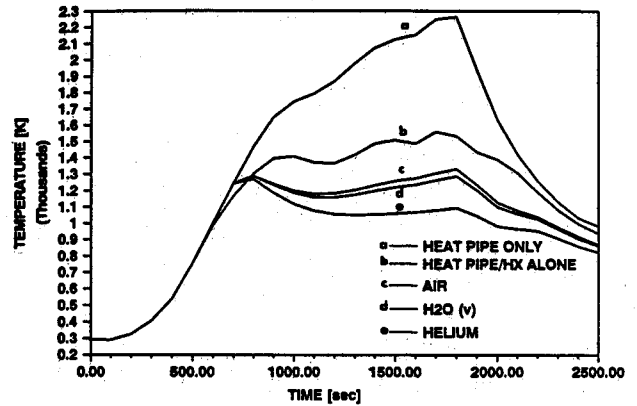


Fig. 10 Transient surface stagnation temperatures using film cooling.

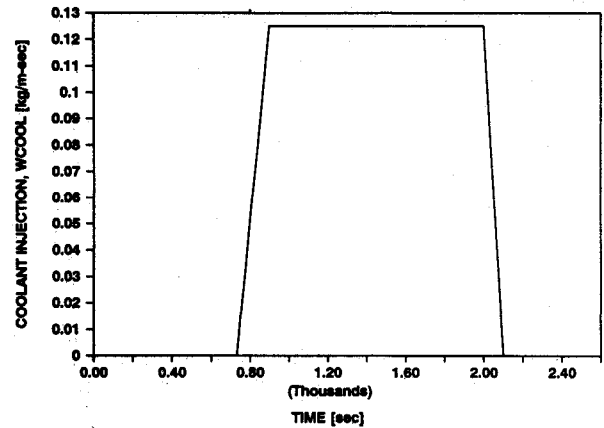


Fig. 11 Film coolant injection profile.

where

$$\dot{w}_{cool} = (\dot{m}/z)_{cool} \quad (26)$$

The results of incorporating the film cooling model with the existing heat pipe-cooled leading-edge finite difference model are shown in Fig. 10. In this figure predicted transient surface stagnation temperatures for three gaseous coolants injected along the leading-edge stagnation line, with no internal heat exchanger, are given. For comparison, the stagnation temperature results for heat pipe cooling alone (no heat exchanger, no mass transfer cooling) and heat pipe with heat exchanger (no mass transfer cooling) are again indicated. The injected coolant mass flowrate per unit span length  $\dot{w}_{cool}$ , used in this study is shown in Fig. 11. The internal heat exchanger heat load used was the same as for the transpiration cooling study (Fig. 9). Using the criteria of the maximum allowable surface temperature of available aero-structural materials as being approximately 1500–1800 K, it appears that under the conditions which yield the results of Fig. 10, heat pipe cooling supplemented by a coolant film injected at the leading edge stagnation line is fully adequate.

Despite the apparent protection the laminar film cooling provides, it has been reported that excessive upstream coolant injection may destabilize the laminar boundary layer, leading

to premature transition and subsequent heat transfer rates in excess of the no-injection laminar values.<sup>34-36</sup> For the range of values of  $\dot{w}_{cool}$  used in the experimental work of Redeker and Miller<sup>29</sup> (see Table 2) very little coolant film mixing with the freestream flow was reported over a surface distance of 16.6 in. The values of  $\dot{w}_{cool}$  used in this study, under similar conditions, falls within this range. Consequently, this potential instability condition was not considered here, and it has been assumed that the coolant forms a discrete laminar film over the leading-edge surface.

It is important to also note that from 0–800 s during the ascent mission described by Figs. 2, 3, and 6 the heat pipe would actually exhibit the startup effects of working fluid melting, vaporization and transition from free molecular to continuum flow.<sup>14</sup> Although very important considerations in the overall heat pipe design and the subject of numerous studies,<sup>11,13,14</sup> these startup effects were not included in the present cooling model. It has been previously demonstrated that heat pipe cooling alone is fully adequate during the startup period.<sup>14</sup> As demonstrated in Figs. 8 and 10, the time interval where heat pipe cooling alone fails is approximately between 1000–2000 s, when the heat pipe is fully operational. Thus additional cooling is required. The present cooling model allows for the examination of the supplemental effects of surface transpiration for film cooling during this critical, maximum aerodynamic heating period of a hypersonic vehicle leading edge structure.

### Concluding Remarks

The problem of determining the feasibility of cooling hypersonic vehicle leading-edge structures exposed to severe aerodynamic surface heating using heat pipe and mass transfer cooling techniques was addressed in this paper. The description of a numerical, finite difference-based hypersonic leading-edge cooling model incorporating poststartup liquid metal heat pipe cooling with surface transpiration and film cooling to predict the transient structural temperature distributions and maximum surface temperatures of hypersonic vehicle leading edge was presented. It is envisioned that this generalized model could be used as a tool for future hypersonic leading-edge structural cooling design calculations. One application of the model was demonstrated for the transient cooling of a typical aerospace plane wing leading-edge section.

Results of this application indicated that liquid metal heat pipe cooling alone was insufficient for maintaining surface temperatures below an assumed maximum level of 1800 K for approximately one-third of a typical aerospace plane ascent trajectory through the Earth's atmosphere. However, by supplementing the heat pipe cooling with an active internal heat exchanger cooling mechanism, with gaseous transpiration cooling along the entire leading-edge length, or with gaseous film coolant injection at the leading-edge stagnation point significant improvements resulted and they appeared to be feasible cooling alternatives. It was also indicated that the injected surface coolant gas possessing the combination of high specific heat and low molecular weight (such as helium in this report) provided the greatest aerodynamic heat transfer reduction to the leading edge surface in both the transpiration and film cooling cases. Hydrogen was not considered a practical coolant gas in this application due to its low combustion temperature (approximately 1100 K) compared to the high maximum allowable leading edge surface temperatures (1500–1800 K).<sup>2</sup>

Additionally, no attempt was made to compare to one another the relative cooling effectiveness of the transpiration and film cooling cases. This would require, among other things, knowledge of the specific mass flow rates necessary to give the heat transfer reduction results presented. Since the surface injection geometry required for these two methods is completely different, as shown in Fig. 5, the coolant injection requirements in the present investigation were developed on a mass flux basis. Therefore, no particular coolant injection

geometry for the hypersonic vehicle leading-edge surface had to be assumed. Rather, emphasis could be placed on determining the feasibility of each cooling concept without concern over what would be the optimum coolant injection design.

It must be further emphasized that the leading-edge cooling model developed by Modlin<sup>6</sup> and described in this paper was designed for use as a tool for further detailed engineering design calculations for poststartup heat pipe/mass-transfer cooling operation. The model's structure was intentionally general in order that it could be applied to a variety of hypersonic vehicle leading-edge systems. As an example, a companion paper prepared by the authors reports the results of a study that considers the problem of cooling SCRAMJET engine inlets using this hypersonic leading-edge cooling model, modified to include type IV shock interaction surface heating effects.

### Acknowledgments

The authors wish to acknowledge the support of the National Science Foundation and the National Aeronautics and Space Administration under several grants.

### References

- <sup>1</sup>McComb, H., Murrow, H., and Card, M., "Structures and Materials Technology for Hypersonic Aerospace Craft," NASA TM-1902583, Jan. 1990.
- <sup>2</sup>McConarty, W., and Anthony, F., "Design and Evaluation of Active Cooling Systems for Mach 6 Cruise Vehicle Wings," NASA CR-1916, 1971.
- <sup>3</sup>Tavella, D., and Roberts, L., "Transpiration Cooling in Hypersonic Flight," Joint Inst. for Aeronautics and Acoustics, JIAA TR-92, June 1989.
- <sup>4</sup>Camberos, J., and Roberts, L., "Analysis of Internal Ablation for the Thermal Control of Aerospace Vehicles," Joint Inst. for Aeronautics and Acoustics, JIAA TR-94, Aug. 1989.
- <sup>5</sup>Silverstein, C. C., "A Feasibility Study of Heat-Pipe-Cooled Leading Edges for Hypersonic Cruise Aircraft," NASA CR-1857, 1971.
- <sup>6</sup>Modlin, J. M., "Hypersonic Aerospace Vehicle Leading Edge Cooling Using Heat Pipe, Transpiration and Film Cooling Techniques," Ph.D. Thesis, Georgia Inst. of Technology, Atlanta, GA, 1991.
- <sup>7</sup>Colwell, G., "Cooling Hypersonic Vehicle Structures," *Proceedings of the 7th International Heat Pipe Conf.*, Minsk, USSR, May, 1990.
- <sup>8</sup>Lees, L., "Laminar Heat Transfer Over Blunt Nosed Bodies at Hypersonic Flight Speeds," *Jet Propulsion*, Vol. 26, April 1956, pp. 259–269.
- <sup>9</sup>Taurer, M., Menees, G., and Adelman, H., "Aerothermodynamics of Transatmospheric Vehicles," *Journal of Aircraft*, Vol. 24, No. 9, 1987, pp. 594–602.
- <sup>10</sup>Chang, W. S., and Colwell, G. T., "Mathematical Modeling of the Transient Operating Characteristics of a Low-Temperature Heat Pipe," *Numerical Heat Transfer*, Vol. 8, 1985, pp. 169–186.
- <sup>11</sup>Colwell, G. T., Jang, J. H., and Camarda, C. J., "Modeling of Startup from the Frozen State," *Proc. Sixth International Heat Pipe Conf.*, Grenoble, France, 1987, pp. 165–170.
- <sup>12</sup>Hendrix, W. A., "The Effect of Body Forces on the Performance of Heat Pipes," Ph.D. Thesis, Georgia Inst. of Technology, Atlanta, GA, 1989.
- <sup>13</sup>Jang, J. H., "An Analysis of Startup From the Frozen State and Transient Performance of Heat Pipes," Ph.D. Thesis, Georgia Inst. of Technology, Atlanta, GA, 1988.
- <sup>14</sup>Morrison, J., "Auxiliary Cooling in Heat Pipe Cooled Hypersonic Wings," M.S. Thesis, Georgia Inst. of Technology, Atlanta, GA, 1990.
- <sup>15</sup>Camarda, C. J., and Masek, R. V., "Design, Analysis, and Tests of a Shuttle-Type Heat-Pipe-Cooled Leading Edge," *Journal of Spacecraft and Rockets*, Vol. 18, No. 1, 1981, pp. 71–78.
- <sup>16</sup>Walton, T., Rashis, B., and Winters, C., "Free Flight Investigations of Subliming Ablators and Transpiration Cooling at Hypersonic Velocities," AIAA Vehicle Design and Propulsion Meeting, Wright Patterson AFB, OH, Nov. 1963, pp. 115–119.
- <sup>17</sup>Roland, H., Pasqua, P., and Stevens, P., "Film and Transpiration Cooling of Nozzle Throats," AEDC-TR-66-88, 1966.
- <sup>18</sup>Dunavant, J., and Everhart, P., "Exploratory Heat Transfer Measurements at Mach 10 on a 7.5 Degree Total Angle Cone Down-

stream of a Region of Air and Helium Transpiration Cooling," NASA TN D-5554, 1969.

<sup>19</sup>Laganelli, A., and Fogaroli, R., "Downstream Influence of Film-Cooling in a High Speed Laminar Boundary Layer," AIAA Paper 71-425, 1971.

<sup>20</sup>Henline, W., "Transpiration Cooling of Hypersonic Blunt Bodies with Finite Rate Surface Reactions," NASA CR-177516, 1989.

<sup>21</sup>Leadon, B., and Scott, C., "Transpiration Cooling Experiments in a Turbulent Boundary Layer at  $M=3$ ," *Journal of the Aeronautical Sciences*, Vol. 23, Jan. 1956, pp. 798-799.

<sup>22</sup>Gollnick, A., "An Experimental Study of Thermal Diffusion Effects on a Partial Porous Mass Transfer Cooled Hemisphere," *International Journal of Heat and Mass Transfer*, Vol. 7, 1964, pp. 699-708.

<sup>23</sup>Parthasarathy, K., and Zakkay, V., "An Experimental Investigation of Turbulent Slot Injection at Mach 6," *AIAA Journal*, Vol. 8, No. 7, 1970, pp. 1302-1307.

<sup>24</sup>Miner, E., and Lewis, C., "A Finite Difference Method for Predicting Supersonic Turbulent Boundary Layer Flows with Tangential Slot Injection," NASA CR-2124, Oct. 1972.

<sup>25</sup>Murray, A., and Lewis, C., "Supersonic Turbulent Boundary Layer Flows with Mass Injection Through Slots and/or Porous Walls," NASA CR-2587, 1975.

<sup>26</sup>Sharpe, L., "Development of Computer Models for Correlating Data of Film Cooling of a Nose Cone under Hypersonic Flow," NASA CR-180673, 1987.

<sup>27</sup>Gross, J., Hartnett, J., Masson, D., and Fazley, C., "A Review

of Binary Laminar Boundary Layer Characteristics," *International Journal of Heat and Mass Transfer*, Vol. 3, 1961, pp. 198-221.

<sup>28</sup>Laganelli, A., "A Comparison Between Film Cooling and Transpiration Cooling Systems in High Speed Flow," AIAA Paper 70-153, 1970.

<sup>29</sup>Redeker, E., and Miller, D., "Mach 16 Film Cooling," *Proc. of the 1966 Heat Transfer and Fluid Mechanics Inst.*, 1966, pp. 387-408.

<sup>30</sup>Hatch, J., and Papell, S., "Use of a Theoretical Flow Model to Correlate Data for Film Cooling or Heating an Adiabatic Wall by Tangential Injection of Gases of Different Fluid Properties," NASA TN D-130, Nov. 1959.

<sup>31</sup>Richards, B., and Stollery, J., "An Experimental Study of the Cooling Effectiveness of a Laminar Two Dimensional Tangential Film in Hypersonic Flow," AIAA Paper 77-703, 1977.

<sup>32</sup>Swenson, B. L., "An Approximate Analysis of Film Cooling on Blunt Bodies by Gas Injection Near The Stagnation Point," NASA TN D-861, Sept. 1961.

<sup>33</sup>Anderson, J., *Hypersonic and High Temperature Gas Dynamics*, McGraw-Hill, New York, 1989, pp. 249-250.

<sup>34</sup>Ledford, O., and Stollery, J., "Film Cooling of Hypersonic Inlets," Imperial College of Science and Technology, I.C. Aero Rept. 72-15, June, 1972.

<sup>35</sup>Starkenber, J., and Cresci, R., "Boundary Layer Transition on a Film Cooled Slender Cone," AIAA Paper 75-194, 1975.

<sup>36</sup>Cresci, R., and Bloom, M., "Hypersonic and Other Viscous Interactions," Polytechnic Inst. of New York, AFOSR-TR-82-0890, June 1982.

## Thermal-Hydraulics for Space Power, Propulsion, and Thermal Management System Design

Recommended Reading from  
Progress in Astronautics  
and Aeronautics

William J. Krotiuk, editor

1990, 332 pp, illus, Hardback  
ISBN 0-930403-64-9  
AIAA Members \$54.95  
Nonmembers \$75.95  
Order #: V-122 (830)

The text summarizes low-gravity fluid-thermal behavior, describes past and planned experimental activities, surveys existing thermal-hydraulic computer codes, and underscores areas that require further technical understanding. Contents include: Overview of Thermal-Hydraulic Aspects of Current Space Projects; Space Station Two-Phase Thermal Management; Startup Thaw Concept for the SP-100 Space Reactor Power System; Calculational Methods and Experimental Data for Microgravity Conditions; Isothermal Gas-Liquid Flow at Reduced Gravity; Vapor Generation in Aerospace Applications; Reduced-Gravity Condensation.

Place your order today! Call 1-800/682-AIAA



American Institute of Aeronautics and Astronautics  
Publications Customer Service, 9 Jay Gould Ct., P.O. Box 753, Waldorf, MD 20604  
Phone 301/645-5643, Dept. 415, FAX 301/843-0159

Sales Tax: CA residents, 8.25%; DC, 6%. For shipping and handling add \$4.75 for 1-4 books (call for rates for higher quantities). Orders under \$50.00 must be prepaid. Please allow 4 weeks for delivery. Prices are subject to change without notice. Returns will be accepted within 15 days.